

# Diurnal profiles of particle-bound ROS of PM<sub>2.5</sub> in urban environment of Hong Kong and their association with PM<sub>2.5</sub>, black carbon, ozone and PAHs

S. Stevanovic<sup>a,f,\*</sup>, N.K. Gali<sup>g</sup>, F. Salimi<sup>d,e</sup>, R.A. Brown<sup>a</sup>, Z. Ning<sup>g</sup>, L. Cravigan<sup>a</sup>,  
P. Brimblecombe<sup>b,h</sup>, S. Bottle<sup>c</sup>, Z.D. Ristovski<sup>a,c</sup>

<sup>a</sup> ILAQH (International Laboratory of Air Quality and Health), Queensland University of Technology, 2 George St, Brisbane, 4000, QLD, Australia

<sup>b</sup> School of Energy and Environment, City University of Hong Kong, Tat Chee Avenue, Kowloon, Hong Kong Special Administrative Region

<sup>c</sup> School of Chemistry, Physics and Mechanical Engineering, Queensland University of Technology (QUT), Brisbane, 4000, QLD, Australia

<sup>d</sup> University Centre for Rural Health – North Coast, School of Public Health, University of Sydney, Australia

<sup>e</sup> Centre for Air Quality & Health Research and Evaluation (CAR), An NHMRC Centre of Research Excellence, Australia

<sup>f</sup> School of Engineering, Deakin University, VIC, 3216, Australia

<sup>g</sup> Division of Environment and Sustainability, The Hong Kong University of Science and Technology Clear Water Bay, Kowloon, Hong Kong

<sup>h</sup> Guy Carpenter Asia-Pacific Climate Impact Centre (GCACIC), School of Energy and Environment, City University of Hong Kong, Hong Kong

## HIGHLIGHTS

- First study investigating diurnal ROS profiles in particle and gas phase and association with diurnal pollutant profiles.
- ROS from both the particle and the gas phase mostly arises from fresh emission sources directly from the traffic.
- ROS decreased with the rise of ozone and particle number, suggesting potential role of ROS in particle growth and aging.
- Quantitative and qualitative ROS gas phase analysis are crucial for assessing the health impacts of atmospheric pollution.
- Nature of anthropogenic gaseous emissions is a very relevant metrics for health implications of various emissions.

## ARTICLE INFO

### Keywords:

PM-Bound ROS  
Urban aerosols  
BC  
Ozone  
Diurnal

## ABSTRACT

Air pollution exposure is associated with a range of adverse health effects, including cardiovascular and respiratory diseases. Particle-bound ROS has been recognised as one of the prevailing parameters to indicate the toxic potential of airborne particulate matter (PM). The temporal variability of particle-bound ROS is a very important metric crucial for the improvement of public health and risk assessment policies. To our knowledge this is the first study aiming to investigate diurnal ROS profiles in both the particle and gas phase and associate them with diurnal variations of important pollutants. For that purpose, we have successfully applied a new instrument to continuously monitor diurnal ROS profiles at two locations in Hong Kong: a busy roadside and an urban background. Data was collected over both the working week and during weekends. We have observed a high correlation between particle-bound ROS and lower concentrations of black carbon (BC) at the roadside during the working week. These associations were less significant over the weekend and at all times with ozone. Our results suggest that most of the particle-bound ROS from both the particle and the gas phase arises from fresh emission sources directly from the traffic. A very interesting observation came out as a result of this study where measured ROS concentration was decreasing with the rise of ozone in conjunction with particle number, suggesting potential role of ROS in particle growth and aging.

## 1. Introduction

Epidemiological studies have associated exposure to particulate matter (PM), particularly fine and ultrafine PM, with adverse health

effects, including cardiovascular and respiratory diseases such as asthma, bronchitis and myocardial infarction (Ristovski et al., 2012; WHO, 2002; Donaldson et al., 2005). The most credible and widely accepted proposed biological mechanism by which PM exposure leads to

\* Corresponding author. School of Engineering, Deakin University, 75 Pigdons Road, Waurin Ponds, 3216, Australia.

E-mail address: [svetlana.stevanovic@deakin.edu.au](mailto:svetlana.stevanovic@deakin.edu.au) (S. Stevanovic).

<https://doi.org/10.1016/j.atmosenv.2019.117023>

Received 5 April 2019; Received in revised form 25 September 2019; Accepted 29 September 2019

Available online 1 October 2019

1352-2310/© 2019 Published by Elsevier Ltd.

observed negative health outcomes is through oxidative stress and inflammation (Nel, 2005; Araujo and Nel, 2009). Hypothesised pathways for PM-induced oxidative stress start with the generation of new reactive oxygen species (ROS) within cells and tissues, that can be brought into the cell with particles or generated in vivo by target cells (such as epithelial cells or macrophages) upon the introduction of PM (Solomon, 2011; Tao et al., 2003). Particle-bound ROS is a metric used to quantify the ROS content of ambient particles, which can be used as a health-based indicator for particulate toxicity. It has been shown that the organic components of PM, or more precisely the oxygenated fraction of PM, described as oxygenated organic aerosols (OOA), act as carriers of particle-bound ROS (Biswas et al., 2007, 2009; Miljevic et al., 2010; Vaughan et al., 2015). Black carbon, also plays an important role as it can act as a carrier of transition metals and semi-volatile components (Hedayat et al., 2015). It is anticipated therefore that most of the ROS-generating reactions occur on PM surfaces that are rich in oxygenated groups and reactive moieties.

Both cellular and acellular assays have been developed to measure potential of PM to cause negative health effects. Although acellular assays have limited physiological relevance lacking direct simulation of actual PM-cell interaction and related immune response, they are typically much more practical to use with fast data readouts and easy implementation. Furthermore, they do not require strictly controlled environments and are easily adaptable to sampling at different locations from various sources. Most commonly used cell-free, molecular probes for the measurement of particle-bound ROS are dichloro-dihydro-fluorescein diacetate (DCFH-DA) and 9,10-bis (phenylethynyl)anthracene-nitroxide (BPEAnit). All of these approaches have certain limitations and are not officially adopted for the measurement of particle-bound ROS (Hedayat et al., 2015). BPEAnit is more robust and stable as it is less prone to auto-oxidation and is not photo sensitive, which is a problem encountered when working with DCFH-DA. Probe stability is crucial when it comes to the employment of the system for unattended real-time measurements. Another very important difference among these molecular probes is their chemical selectivity. DCFH is sensitive towards organic peroxides, hydroperoxides, aldehydes, alcohols and hypochlorite. Finally, BPEA-nit traps carbon-centered, nitrogen-centered and sulphur-centered radicals, peroxy and hydroxyl radicals (if the reaction is done in dimethyl sulfoxide (DMSO)), which provides a broader spectrum of detectable species that are considered relevant for particulate toxicity (Hedayat et al., 2015).

Several online systems have been developed to monitor the particle-bound ROS of airborne PM (Table 1).

Among them, several prototypes were designed to work with DCFH. Wang et al. (2011) used a particle into liquid sampler (PILS) approach for particle collection. This instrument's working principle is based on condensational particle growth and subsequent collection of enlarged particles by a wetted cyclone or an impactor. King and Weber (2013) designed a mist chamber that traps both the gas and particles that are then being analysed automatically. Improved version of this system has been proposed by Wragg et al. (2016) who reported better time resolution and improved sampling methodology. The latest version of this system has been described by Zhou et al. (2017). Problems with these approaches are mainly related to the usage of DCFH and HRP and issues with auto-oxidation (Chen et al., 2010) which can lead to an

overestimation of OP (Pal et al., 2012). To overcome this problem, some researchers utilized DTT as a part of the system (Eiguren-Fernandez et al., 2017; Stevanovic et al., 2012).

Current systems designed for the online monitoring of particle-bound ROS are all limited in their time resolution by the ~10 min reaction time of the DCFH-DA probe required for accurate detection of ROS species. This is evidenced by the time resolution for these systems being 8, 10, 10.5, 12 and 20 min for the ROS Analyser (Zhou et al., 2018), ROS Sampling-Analysis Systems (Venkatachari and Hopke, 2008), OROSS (King and Weber, 2013), the Online Particle-bound ROS Instrument (OPROSI) (Wragg et al., 2016; Fuller et al., 2014) and the GAC-ROS (Huang et al., 2016), respectively. This comparatively long collection times make these systems less effective for atmospheric measurements, as many short-lived free-radical species will not survive to be directly assessed by the methodology. Another limitation of some current automated ROS monitors is the effective concentration of the liquid samples collected. The GAC-ROS and PINQ systems generate a highly concentrated sample due to their high ratios of aerosol to liquid sample flow-rates. The OROSS system is not a continuous flow system, but generates a highly concentrated sample through collecting PM with a high flow-rate into a small liquid volume over several minutes. In comparison, the two PC-based systems are continuous flow systems with significantly lower aerosol to liquid flow ratios, resulting in an approximately order of magnitude lower in sample concentration. The consequence of this is that the PC-based systems have an order of magnitude higher LOD than other systems. This is significant as a lower LOD facilitates the detection of OP and particle-bound ROS at lower ambient levels. The PINQ's combination of: low LOD; high time resolution; and unique ability to also measure the water-insoluble PM fraction; provides a new and more sensitive instrument for PM-bound ROS measurements. The temporal variability of particulate toxicity is a very important metric that remains to be fully investigated. Having a reliable technique that can measure this parameter would significantly improve risk assessment policies and help in determinations of the actual impact of air pollution on public health.

To our knowledge, there have been only three attempts in the literature to measure online diurnal OP profiles (Wang et al., 2011; Wragg et al., 2016; Huang et al., 2016; Puthussery et al., 2018). Of these, Wragg et al. had the best time-resolution for the measurements, however, as discussed above, they employed a DCFH-based approach which was impacted by sensitivity and stability factors. Huang et al. (2016) reported only daily averages while Fueller et al. (Fuller et al., 2014), used a similar approach to that of Wragg et al., but with a smaller sampling flow rate (5 lpm). Puthussery et al. employed the DTT assay with a time resolution of 1 h (Puthussery et al., 2018). None of these systems was able to monitor diurnal profiles of OP contained in both the gas and particle phase.

To address this significant gap in our knowledge of real-time PM characteristics, we have employed a modified and improved version of PILS, a novel particle into liquid quencher (PINQ), that uses BPEAnit for the detection of ROS derived from both particles and gas phase. This PINQ system samples 16.7 lpm of air and collects the sample for 3 min, while the detection response is effectively immediate. We successfully employed this new instrument to continuously monitor diurnal ROS profiles at two locations in Hong Kong: a busy roadside and an urban

**Table 1**  
(Stevanovic) List of online ROS instruments and their key characteristics.

Instrument	Chemical Assay	Collection Method	Water -Insoluble Particles	Sample Flowrate	Time Resolution	Limit of Detection
ROS Sampling-Analysis System	DCFH	PILS	No	16.7 Lpm	10 min	n/a
OPROSI	DCFH	PC	No	5 Lpm	≤12 min	4 nmol m <sup>-3</sup>
GAC-ROS	DCFH	GAC	No	16.7 Lpm	20 min	0.12 nmol m <sup>-3</sup>
ROS Analyser	DCFH	PC	No	1.7 Lpm	8 min	2 nmol m <sup>-3</sup>
OROSS	DCFH	MC	No	20 Lpm	10.5	0.15 nmol m <sup>-3</sup>
PINQ	BPEA-nit	IAC	Yes	16.7 lpm	1 min	0.08 nmol m <sup>-3</sup>

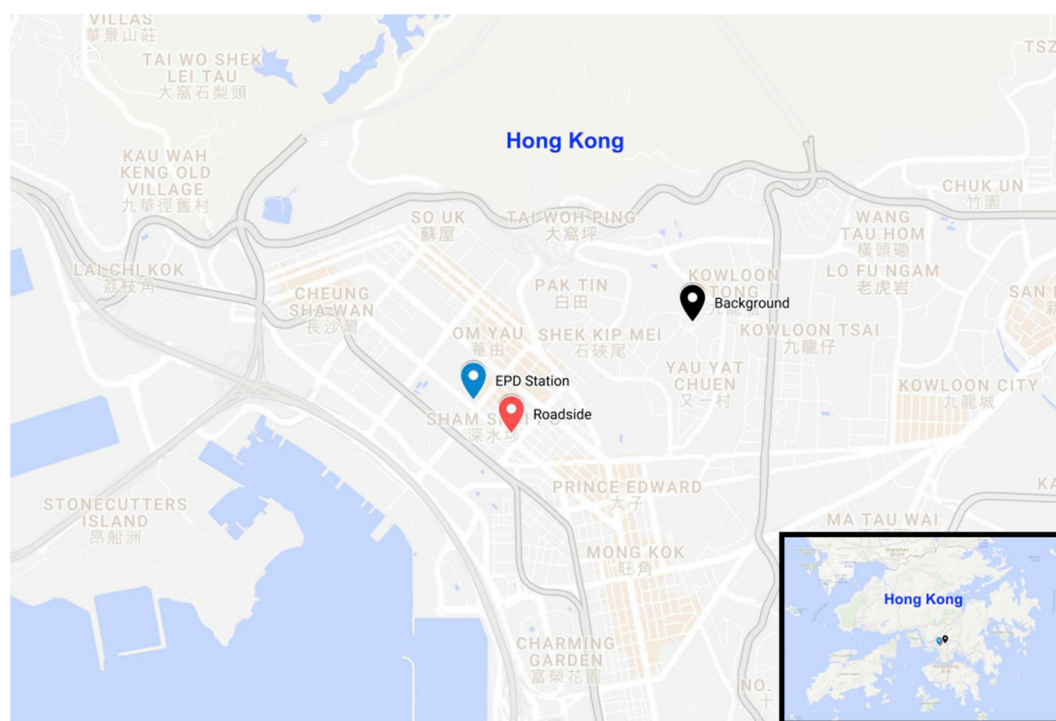


Fig. 1. (Stevanovic). Location of sampling sites in Hong Kong.

background, collecting data over both the working week and during weekends. This was the first time diurnal profiles of both the gas phase and particulate OP were presented in the literature and that the diurnal profiles of OP were associated with the diurnal variations of important pollutants.

## 2. Materials & methods

### 2.1. Sampling strategy

In this study, air quality monitoring was conducted at two sampling sites, each representing roadside and urban background, both located within 1.5 km range. These two sites are referred as roadside and rooftop throughout the manuscript. The details of these locations are as shown in Fig. 1. The typical roadside site was located at about 5 m away from the kerb on the Lai Chi Kok (LCK) road in Sham Shui Po, Kowloon, Hong Kong where fresh emissions from traffic sources are dominant. In addition, monitoring was undertaken at the Kowloon Tong (KLT) district, which represents a typical urban ambient environment with well mixed and aged aerosols distant from traffic sources. A  $PM_{2.5}$  inlet was specifically designed for 16.7 lpm flow rate. This flow rate was used for

online measurements of reactive oxygen species (ROS) across 24 h. The ROS was measured online using PINQ once in every 2 h over a period of 24 h each day. It is repeated for 6 days, though on alternate days, spanning 2 weeks at each sampling location, thus comprising 4 week-days and 2 weekends. The sampling periods were 12 Sep 2016–25 Sep 2016 at roadside site, and from 6 Oct 2016–17 Oct 2016 at the urban background site.

### 2.2. PILS set-up and ROS analysis

The PINQ was designed and built in-house at Queensland University of Technology (QUT), Brisbane, Australia. A diagram of the instrument is shown below (Fig. 2).

The PINQ was designed to draw aerosol at a flow rate of 16.7 lpm. A primary aspect of the design of the PINQ was to employ a condensational growth chamber to mix the incoming  $PM_{2.5}$  aerosol with a stream of water vapour sufficient to create supersaturation conditions which then causes the water vapour to condense onto the particles inside the aerosol, exponentially growing them into a bigger size. The resultant condensed aerosol then enters the liquid vortex cyclone in the cone. A stream of captured liquid is continuously introduced at the top of the

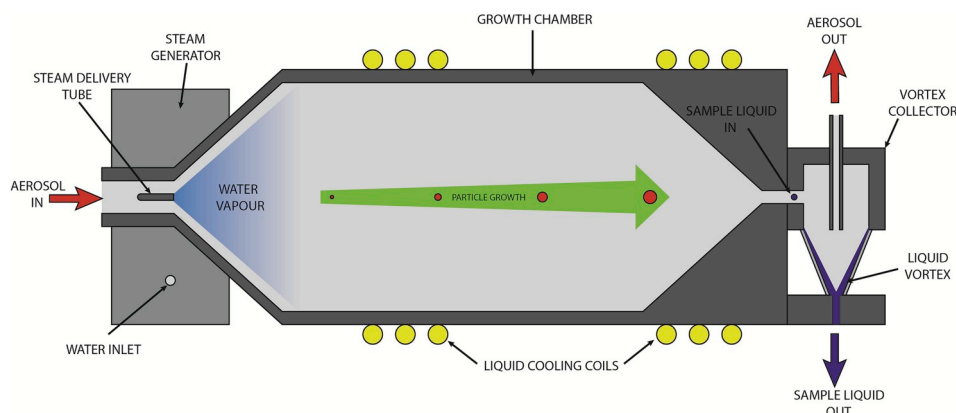


Fig. 2. (Stevanovic). Sketch of PINQ.

cone and pumped out at the base. At this point a profluorescent nitroxide probe 9-(1,1,3,3-tetramethylisindolin-2-yloxy)-5-ethynyl-10-(phenylethynyl) anthracene, termed as BPEAnit, at  $0.8 \mu\text{M}$  in DMSO was continuously introduced at a rate of  $0.28 \text{ ml min}^{-1}$ , to react with the condensed aerosol particles in the liquid vortex cyclone and to capture ROS. The reacted liquid was then collected at the same rate of  $0.28 \text{ ml min}^{-1}$  and analysed spectrofluorometrically, using in-line fluorometers with USB2000 + and Spectra Suite software, following the fluorescence emission at  $484.79 \text{ nm}$  using excitation at  $430 \text{ nm}$ . A calibration curve created from  $10 \text{ nM}$  to  $200 \text{ nM}$  concentrations of BPEAnit-Methyl (a representative fully fluorescent probe-adduct species) was used to convert the fluorescence intensity generated in the sample into units reflecting ROS activity as per our previous studies (Stevanovic et al., 2012a, 2012b).

### 2.3. Description of PINQ

The PINQ is a steam collection device designed for the solubility independent collection of ultrafine particles into the BPEAnit ROS assay. The system mixes incoming air with flow of steam inside an expanding cone, creating a supersaturated mixture in which particles undergo condensational growth, increasing them in size to above  $1 \mu\text{m}$  for efficient collection. The steam temperature at the point of injection is at a maximum of  $105^\circ\text{C}$ . However, the expansion of the steam exiting the tube and corresponding mixing with the aerosol leads to a rapid drop in temperature down to approximately  $40^\circ\text{C}$  after the expansion cone. Only a small fraction of the aerosol will be exposed to the high temperature steam at its exit point. This, combined with the rapid cooling of the aerosol, leads to an expectation that its influence on ROS measurements will be minimal.

PM is collected directly into the BPEAnit assay inside a vortex collector. This device is similar to a miniature PM cyclone, with the internal shape and dimensions of the device creating a spinning column of air inside a cone. Where the vortex collector differs is that while the device is operating, a liquid supply is continuously injected at the top of the cone and removed at the base. As the liquid passes down the cone, the force of the rotating air causes the liquid to spread up the walls of the cone, creating a spinning liquid vortex. In the case of the PINQ, the collection liquid used is a solution of BPEAnit in DMSO. Grown particles entering the collector are deposited into the liquid, where ROS present on the particle undergo a diffusion-limited reaction with the probe to create a fluorescent product. More details on the BPEAnit probe can be found in Stevanovic et al. (2012)

The vortex collector also captures some gas-phase ROS through a mechanism which is not entirely understood. In order to measure particle phase ROS, both filtered and unfiltered aerosol samples are taken. The filtered sample represents the gas phase ROS contribution, which is subtracted from the unfiltered sample to ascertain particle phase ROS concentrations. As the gas phase collection efficiency of the instrument is currently unknown, gas phase measurements shown in this manuscript are semi-quantitative. The PM collection efficiency of the device is  $<95\%$  for insoluble PM, with a cut-off size of  $30 \text{ nm}$ .

All liquid flows are regulated through the use of a peristaltic pump. Tubing is regularly changed to ensure stable liquid flowrates. The instrument was operated offline, with  $3 \text{ mL}$  liquid samples of filtered and unfiltered aerosol collected every  $2 \text{ h}$  for analysis. The collection time of each sample was  $3 \text{ min}$ , with an additional minute between collection and measurement inside a portable fluorometer. A real time variant of the instrument is currently under development. More details on the instrument performance characteristics (collection efficiency, response time, steam dilution factor and level of detection) can be found in Brown et al. (Reece et al., 2018).

### 2.4. Co-pollutant collection system and EPD data acquisition

Co-pollutants such as particulate black carbon (BC) and polycyclic

aromatic hydrocarbons (PAHs) were collected in-line with ROS analysis employing AE33/AE51 methodology (3lpm, Magee) and PAS2000 methodology (1.6lpm, EcoChem) respectively. The aerosol particle concentration and the size distribution was determined using SMPS with DMA 3081 ( $0.3 \text{ lpm}$ , TSI). In addition, the measured concentrations of  $\text{O}_3$  and  $\text{PM}_{2.5}$  were acquired from the Environment and Protection Department, Govt. of Hong Kong SAR (HKEPD) monitoring station located at Sham Shui Po, which is also within the range of  $1.5 \text{ km}$  of two sampling sites as described above and as shown in Fig. 1.

### 2.5. Statistical analysis

We initially employed box-and-whisker plots to visualise the diurnal trends of pollutants at each location. Solid dashed line inside the box represents the mean value, each box includes the interquartile range (IQR), and whiskers show the minimum and maximum values. Individual points refer to the outliers which are  $1.5 \text{ IQR}$  higher (lower) than  $3 \text{rd}$  quartile ( $1 \text{st}$  quartile). Associations between each pollutant and the ROS were estimated using linear regression models,  $p$  values were reported as  $<0.001$ ,  $<0.01$ ,  $<0.05$  and  $>0.05$ . Estimate refers to the change in ROS per a unit increase in each pollutant concentration.

## 3. Results and discussion

### 3.1. Diurnal profiles of particulate and gaseous ROS

Fig. 3 displays the diurnal profiles of particle-bound ROS measured in gaseous and particulate phase at two sampling sites, one representing busy, urban street setting and the other one measured at urban background. Particle-bound ROS was normalised by the volume of air sampled, which depicts the exposure upon inhalation of ambient particles much better than the mass normalised OP, specifically as the value expressed in this way includes the influence of some other factors such as temperature, humidity and wind intensity. As we can see from diurnal profiles, ROS measured in the gas phase is having strong positive association with the particle phase at roadside and at the rooftop, which can be attributed to the partitioning of species between these two phases (Stevanovic et al., 2017). Trends in  $\text{PM}_{2.5}$  follow the trends of particle phase particle-bound ROS.

Diurnal trend of particle-bound ROS in the particle phase follows the trend expected for roadside sites. In the morning rush hour ( $6:00\text{--}8:00$ ), it increases, peaks at  $10:00$ , after which it slowly decreases and then increases again during an afternoon peak hour ( $15:00\text{--}16:00$ ). Diurnal changes of particle-bound ROS reflect the diurnal changes of  $\text{PM}_{2.5}$ . Interestingly, after the ROS concentration decreases in the evening, it peaks again at  $22:00$ .  $\text{PM}_{2.5}$  concentration also reaches its highest diurnal level at this time. At first, this result may look surprising, taking into account that the traffic intensity as well as contribution of all the sources is at its lowest point late in the evening. By taking a closer look at the meteorological data for this region and this time of the year, it can be seen from Fig. 4 that the height of the boundary layer (BL) approaches its lowest point at  $22:00$ . A lower BL height results in increased aerosol concentrations as emissions dilute to a smaller volume (Petäjä et al., 2016). As a consequence, particulate particle-bound ROS increased by  $40\%$  in the late evening, following the raising concentration of pollutants. In general, the BL height correlates well with temperature (Mehta et al., 2017), this can also be exploited to examine diurnal trends in pollutant concentrations, which are product of both emissions and transport in the BL.

### 3.2. contribution of primary and secondary pollution to the measured particle-bound ROS

Significant association was observed between  $\text{PM}_{2.5}$  and particle-bound ROS during the weekdays, when the traffic intensity was high, at both sites. There is no significant association observed over the



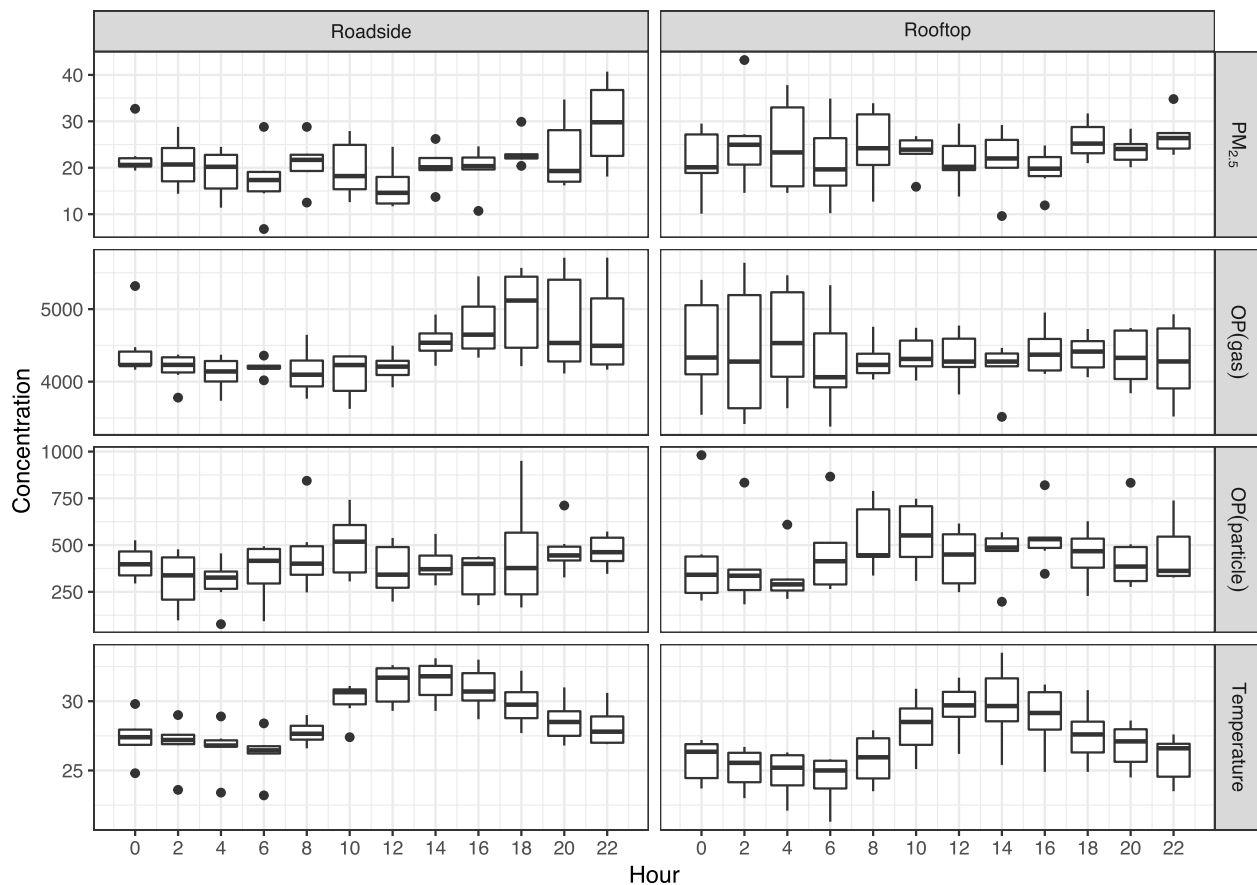


**Fig. 3. (Stevanovic).** Diurnal  $PM_{2.5}$  [ $\mu g \cdot m^{-3}$ ], particle-bound ROS [ $nmol \cdot m^{-3}$ ] and temperature [ $^{\circ}C$ ] profiles measured in particulate and gaseous phase and averaged over the sampling period at two sampling locations, busy roadside and rooftop as an urban background site.

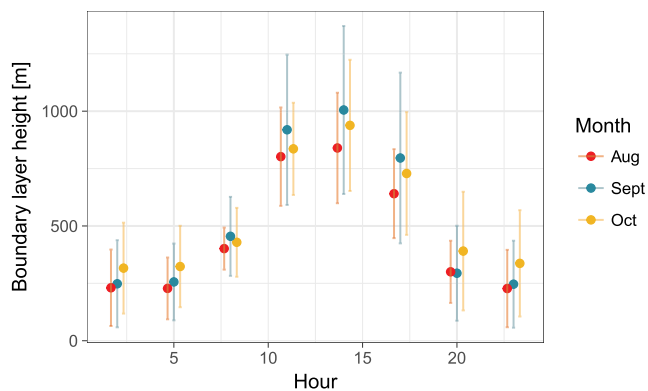


**Fig. 4. (Stevanovic)** Diurnal variation of the height in boundary layer during August, September and October 2016 when the measurements were conducted. The data is based on reanalysis data from ERA Interim, taken for the closest grid (approximately 13 by 13 km) to Hong Kong, at 22.375  $^{\circ}N$  and 114.125  $^{\circ}E$ .

weekend.

BC associates well with the measured ROS concentration in the particle phase at the rooftop, but shows no associations at the roadside. This may be due to high concentration of BC at the roadside. If the concentration of BC was too high, measurement of particle-bound ROS can be skewed as high concentrations of collected particles causes light scattering during the fluorescence measurements and the value measured and thus reported here, is most certainly underestimated. This is apparent from Fig. 5 where we can see a reasonable correlation at the roadside during weekdays for concentrations lower than 3000  $ng \cdot m^{-3}$ .

For concentrations above that the fluorescence signal decreases due to scattering and gives a false low particle-bound ROS concentration.

Furthermore, PAHs associated with the particle-bound ROS only at the rooftop during the weekend, while the ozone shows a significant association at the rooftop during the workdays (see Table 2).

Similarly, in Table 3 associations between  $PM_{2.5}$ ,  $O_3$ , BC and PAH with particle-bound ROS of gas phase are shown. It can be seen that  $PM_{2.5}$  is having good positive association with the ROS concentration measured in the gas phase at both sampling locations during the workdays, which was also observed for the particle phase. The particle-bound ROS of gaseous phase cannot be directly linked to the species contained in  $PM_{2.5}$ , but this observation may indicate that the ROS measured in both the particle and gas phase may originate from the same source. This can be further supported by the association with BC at both sites (Fig. 6). High association with BC means that most of the reactive species are coming from the traffic measured at both sites during the weekdays when the traffic intensity was high. During the weekend, this association is also significant at both the rooftop and roadside measurement sites. This pattern may indicate that even during the weekend, the majority of the pollution measured arises from the transportation sources. High concentrations of BC do not influence gas phase measurements as the inlet air flow was filtered prior to entering the PINQ.

Ozone was measured at the EPA station that was around 1.5 km distant from both measurement sites. We have assumed that the distribution of ozone was homogenous across this distance and that the air was mixed through a boundary layer during the day. The location of the monitoring station means that any street canyon effect will not be represented by the ozone measurements.

Ozone associates well only with the gaseous ROS measured at the

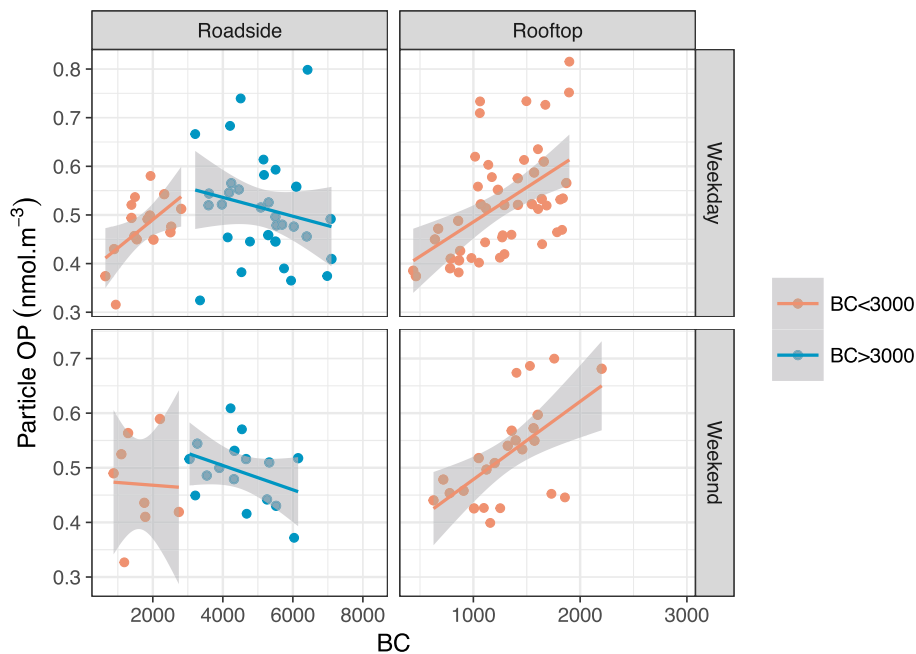


Fig. 5. (Stevanovic). Relationship between particle-bound ROS measured in particle phase and BC concentration lower and higher than 3000 ng/m<sup>3</sup>.

Table 2  
(Stevanovic) Statistical interpretation of correlation between particle-bound ROS of PM on the roadside and rooftop with PM<sub>2.5</sub>, O<sub>3</sub>, BC and PAH during weekdays and weekend.

Particles	Rooftop (background)			Roadside		
	R <sup>2</sup>	estimate	p value	R <sup>2</sup>	estimate	p value
PM <sub>2.5</sub>	0.34	16.35	<0.001	0.27	13.68	<0.001
	0.06	7.62	>0.05	0.00068	-0.531	>0.05
BC	0.26	0.26	<0.001	0.016	0.012	>0.05
	0.35	0.26	<0.01	0.00009	0.00075	>0.05
PAH	0.01	-18.03	>0.05	0.00296	0.289	>0.05
	0.28	108.9	<0.01	0.000558	-0.352	>0.05
O <sub>3</sub>	0.13	2.82	<0.05	0.022	0.77	>0.05
	0.00	-0.255	>0.05	0.000008	0.016	>0.05

Table 3  
(Stevanovic) Statistical interpretation of correlation between particle-bound ROS of gas phase on the roadside and rooftop with PM<sub>2.5</sub>, O<sub>3</sub>, BC and PAH during weekdays and weekend.

Gas	Rooftop (background)			Roadside		
	R <sup>2</sup>	estimate	p value	R <sup>2</sup>	estimate	p value
PM <sub>2.5</sub>	0.43	45.87	<0.001	0.23	36.88	<0.001
	0.14	35.10	>0.05	0.255	23.16	<0.05
BC	0.33	0.72	<0.001	0.012	0.032	>0.05
	0.29	0.69	<0.01	0.353	0.107	<0.01
PAH	0.03	-71.01	>0.05	0.027	8.813	>0.05
	0.04	-124.3	>0.05	0.25	17.61	<0.05
O <sub>3</sub>	0.04	3.95	>0.05	0.0003	0.26	>0.05
	0.26	12.63	<0.05	0.085	3.743	>0.05

rooftop over the weekend, showing that a portion of ROS measured is due to secondary pollution, where the primary VOCs are oxidised by ozone, UV or reactive radicals. This result indicates that the particle-

bound ROS measured at selected sites in Hong Kong originates mainly from primary pollution and that the contribution of secondary pollutants, hereby presented by ozone concentrations, is limited.

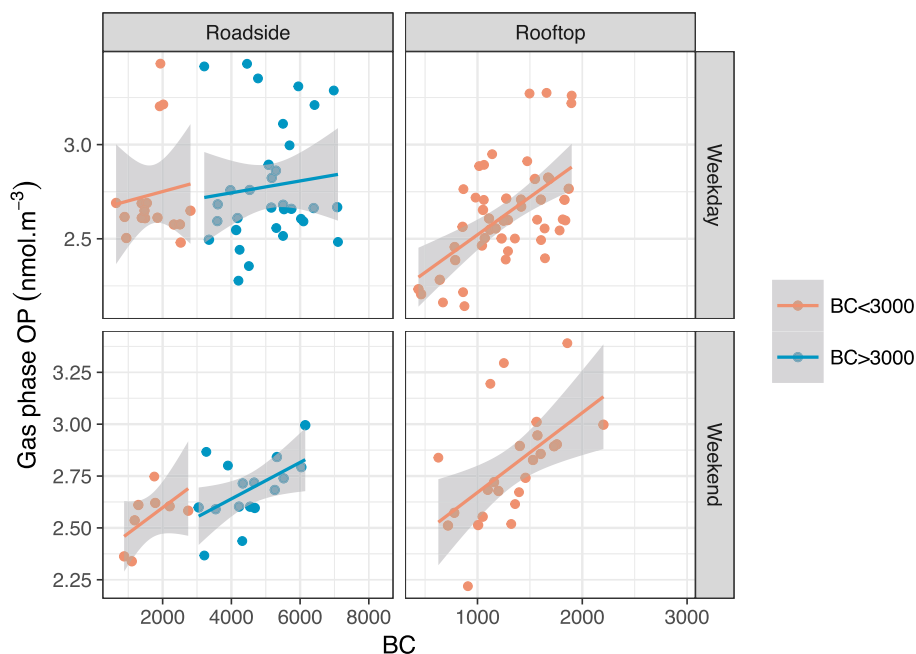


Fig. 6. (Stevanovic) Relationship between particle-bound ROS measured in gas phase and BC concentration lower and higher than 3000 ng/m<sup>3</sup>.

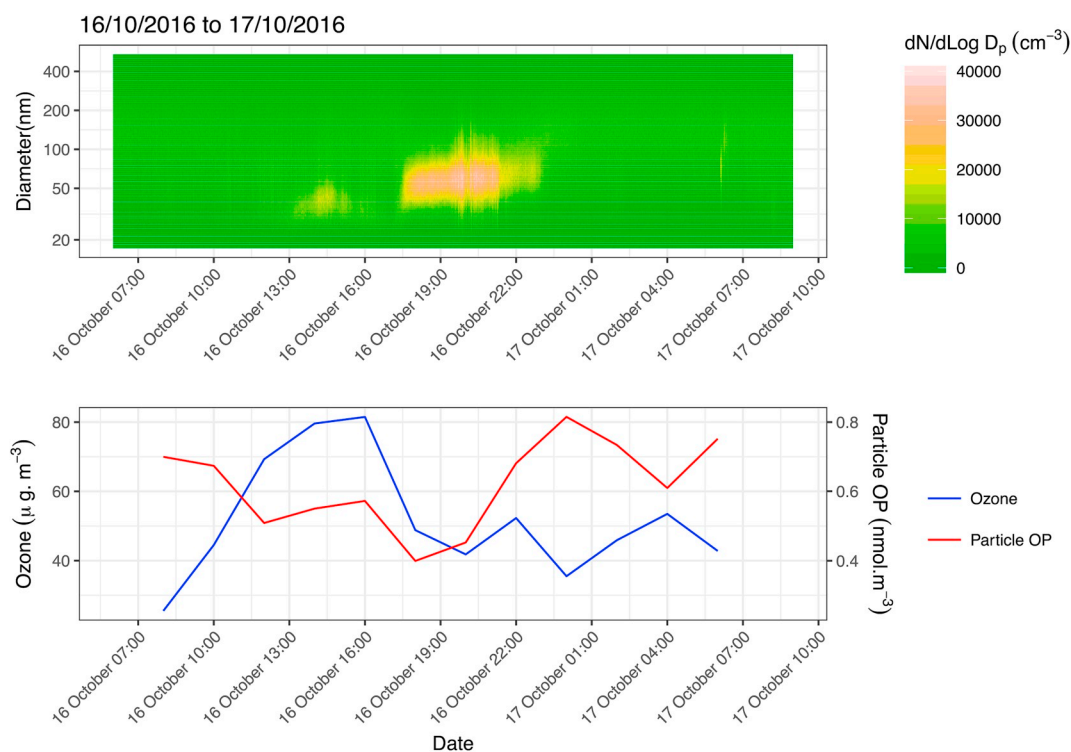
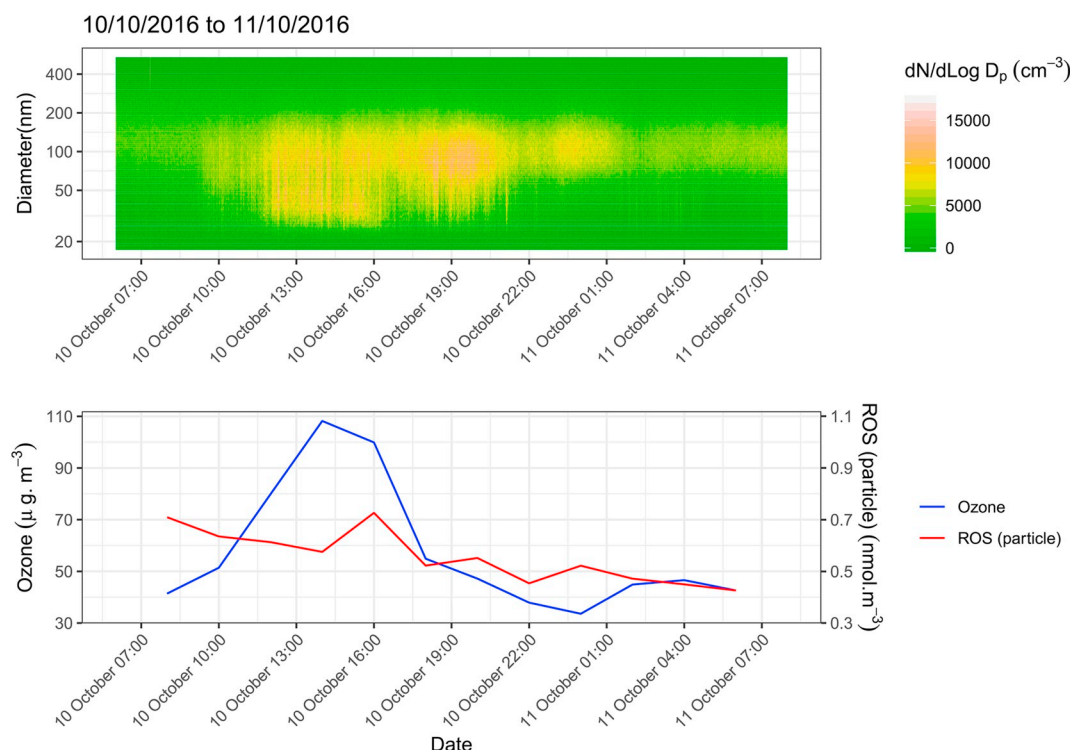


Fig. 7. (Stevanovic) Time series of the particle number size distributions, ozone concentration and particle-bound ROS measured in particle phase on the busy roadside.

Figs. 7 and 8 provide a more detailed analysis of the data sampled from the rooftop for a typical weekday and over a weekend respectively. It is evident that there is an appearance of recently nucleated particles at certain times (12:00–14:00) for both days. New particles observed have diameters lower than 50 nm and cannot be associated with any stationary or mobile source nearby as these events were random and short-living. Based on their size (20–50 nm), it may be that the particle formation happened further from the measurement site and that the particles were transported to the rooftop. By looking at the UV intensity

(UVI) indexes, at the time when new particles were detected, it is unlikely that a new particle formation (NPF) event could happen nearby at this time due to UVI values that were 40–50% lower than at earlier times of the day (decreasing from ~8 in the morning to between 2 and 3 at noon) on both days.

Ozone concentrations rise through the day along with the detection of new particles at the site. This further supports the hypothesis that a potential earlier NPF happened further from the rooftop and was then transported there. To further support the prospect that the particles



**Fig. 8. (Stevanovic)** Time series of the particle number size distributions, ozone concentration and particle-bound ROS measured in particle phase measured at the urban background site.

detected did not originate from usual primary sources, such as traffic, BC concentrations at these times decrease whilst ozone and particle numbers increase. This is usually taken as an indication that newly observed particles are most likely secondary-sourced.

Interestingly, at the same time as ozone levels rise in conjunction with particle number, measured ROS concentrations decrease. We do not have an adequate explanation for this observation which logically reflects an overall lower surface reactivity from these particles. However, it is potentially a significant result that only comes to light through the use of the rapid, real-time monitoring methodology employed here. Further studies are necessary to understand the detailed influence of ROS during particulate growth and aging in this context. The low particle-bound ROS result may arise from the depletion of ROS used for secondary transformation of primary particles, or it may mean that these particles are transformed to have decreased particle-bound ROS (as measured by our technique).

In summary, measured ROS profiles were compared with diurnal changes in  $\text{PM}_{2.5}$ , BC,  $\text{O}_3$  and PAHs. It was found that particle-bound ROS in the particle phase associates well with  $\text{PM}_{2.5}$  and with lower concentrations of BC at the roadside during the working week. These associations were less significant over the weekend, perhaps reflecting the influence of aged particles and transport factors. As profiles of  $\text{PM}_{2.5}$  and BC were very similar for measurements taken at a busy roadside site, it was concluded that the traffic was the main source of PM. Higher associations between particle-bound ROS and primary pollutants as well as less significant associations with ozone, used as a marker for secondary pollutant formation, indicated that most of the particle-bound ROS from both particle and gas phase pollution arises from fresh emissions sources directly from nearby traffic.

#### Author contributions

S.S Made the experimental design, Made experimental set-up, performed data analysis and wrote the manuscript.

N. K. G Conducted measurements; Assisted with the experimental

design and set up; reviewed the manuscript.

F. S Prepared Figs. 3–8, Modelled the data, Reviewed manuscript.

R. A. B Assisted with experiments, Finalised the design of PINQ device, Reviewed the manuscript.

L. C Assisted with the data interpretation, reviewed the manuscript.

Z. N Reviewed the manuscript, contributed to the experimental design and data interpretation.

S.B Reviewed the manuscript, contributed to the experimental design and data interpretation.

Z.R Came up with the original idea, contributed to the experimental design, assisted with data interpretation; reviewed the manuscript.

#### Declaration of competing interest

The authors declare that they have no known competing financial interests or personal relationships that could have appeared to influence the work reported in this paper.

#### Acknowledgment

This work was supported by Research Grants Council, Government of Hong Kong (Grant 11204115), Research Grants Council, Government of Hong Kong (Grants 11204115; 11300114) and the Australian Research Council Discovery Grant (DP120100126).

#### Appendix A. Supplementary data

Supplementary data to this article can be found online at <https://doi.org/10.1016/j.atmosenv.2019.117023>.

#### References

- Araujo, J.A., Nel, A.E., 2009. Particulate matter and atherosclerosis: role of particle size, composition and oxidative stress. Part. Fibre Toxicol. 6 (1).
- Biswas, S., et al., 2007. Particle volatility in the vicinity of a freeway with heavy-duty diesel traffic. Atmos. Environ. 41 (16), 3479–3493.



- Biswas, S., et al., 2009. Chemical speciation of PM emissions from heavy-duty diesel vehicles equipped with diesel particulate filter (DPF) and selective catalytic reduction (SCR) retrofits. *Atmos. Environ.* 43 (11), 1917–1925.
- Chen, X., et al., 2010. 2',7'-Dichlorodihydrofluorescein as a fluorescent probe for reactive oxygen species measurement: forty years of application and controversy. *Free Radic. Res.* 44 (6), 587–604.
- Donaldson, K., et al., 2005. Role of inflammation in cardiopulmonary health effects of PM. *Toxicol. Appl. Pharmacol.* 207 (2 Suppl. 1), 483–488.
- Eiguren-Fernandez, A., Kreisberg, N., Hering, S., 2017. An online monitor of the oxidative capacity of aerosols (o-MOCA). *Atmos. Meas. Tech.* 10 (2), 633–644.
- Fuller, S.J., et al., 2014. Comparison of on-line and off-line methods to quantify reactive oxygen species (ROS) in atmospheric aerosols. *Atmos. Environ.* 92, 97–103.
- Hedayat, F., et al., 2015. Review – evaluating the molecular assays for measuring the oxidative potential of particulate matter. *Chem. Ind. Chem. Eng. Q.* 21 (1–2), 201–210.
- Huang, W., et al., 2016. Development of an automated sampling-analysis system for simultaneous measurement of reactive oxygen species (ROS) in gas and particle phases: GAC-ROS. *Atmos. Environ.* 134, 18–26.
- King, L.E., Weber, R.J., 2013. Development and testing of an online method to measure ambient fine particulate reactive oxygen species (ROS) based on the 2',7'-dichlorofluorescein (DCFH) assay. *Atmos. Meas. Tech.* 6 (7), 1647–1658.
- Mehta, S.K., et al., 2017. Diurnal variability of the atmospheric boundary layer height over a tropical station in the Indian monsoon region. *Atmos. Chem. Phys.* 17 (1), 531–549.
- Miljevic, B., et al., 2010. Oxidative potential of logwood and pellet burning particles assessed by a novel profluorescent nitroxide probe. *Environ. Sci. Technol.* 44 (17), 6601–6607.
- Nel, A., 2005. Air pollution-related illness: effects of particles. *Science* 308 (5723), 804–806.
- Pal, A.K., et al., 2012. Screening for oxidative stress elicited by engineered nanomaterials: evaluation of acellular DCFH assay. *Dose-Response* 10 (3), 308–330.
- Petäjä, T., et al., 2016. Enhanced Air Pollution via Aerosol-Boundary Layer Feedback in China, vol. 6, p. 18998.
- Puthussery, J.V., Zhang, C., Verma, V., 2018. Development and field testing of an online instrument for measuring the real-time oxidative potential of ambient particulate matter based on dithiothreitol assay. *Atmos. Meas. Tech.* 11 (10), 5767–5780.
- Reece, A., Brown, S.S., Bottle, Steven E., Ristovski, Zoran D., 2018. An Instrument for the Rapid Quantification of PM Oxidative Potential: the Particle into Nitroxide Quencher (PINQ) Atmospheric Measurement Techniques.
- Ristovski, Z.D., et al., 2012. Respiratory health effects of diesel particulate matter. *Respirology* 17 (2), 201–212.
- Solomon, P.A., 2011. Air pollution and health: bridging the gap from sources to health outcomes. *Environ. Health Perspect.* 119 (4), 156–157.
- Stevanovic, S., et al., 2012. The use of a nitroxide probe in DMSO to capture free radicals in particulate pollution. *Eur. J. Org. Chem.* (30), 5908–5912, 2012.
- Stevanovic, S., et al., 2017. Oxidative potential of gas phase combustion emissions - an underestimated and potentially harmful component of air pollution from combustion processes. *Atmos. Environ.* 158, 227–235.
- Tao, F., Gonzalez-Flecha, B., Kobzik, L., 2003. Reactive oxygen species in pulmonary inflammation by ambient particulates. *Free Radic. Biol. Med.* 35 (4), 327–340.
- Vaughan, A., et al., 2015. Removal of organic content from diesel exhaust particles alters cellular responses of primary human bronchial epithelial cells cultured at an air-liquid interface. *J. Environ. Anal. Toxicol.* 5 (5), 100316-1.
- Venkatachari, P., Hopke, P.K., 2008. Development and laboratory testing of an automated monitor for the measurement of atmospheric particle-bound reactive oxygen species (ROS). *Aerosol Sci. Technol.* 42 (8), 629–635.
- Wang, Y., et al., 2011. Laboratory and field testing of an automated atmospheric particle-bound reactive oxygen species sampling-analysis system. *J. Toxicol.* 2011, 9.
- WHO, 2002. The World Health Report, 2002. Reducing Risks, Promoting Health Life. WHO, Geneva, Switzerland.
- Wragg, F.P.H., et al., 2016. An automated online instrument to quantify aerosol-bound reactive oxygen species (ROS) for ambient measurement and health-relevant aerosol studies. *Atmos. Meas. Tech.* 9 (10), 4891–4900.
- Zhou, J., et al., 2017. Development, Characterization and First Deployment of an Improved Online Reactive Oxygen Species Analyzer, pp. 1–27.
- Zhou, J., et al., 2018. Development, characterization and first deployment of an improved online reactive oxygen species analyzer. *Atmos. Meas. Tech.* 11 (1), 65–80.